

## Chapter 11

# CELLULAR AND SUBCELLULAR ANALYSIS ON CHIP

Hang Lu<sup>1</sup> and Klavs F. Jensen<sup>2</sup>

<sup>1</sup>*Department of Anatomy, University of California, San Francisco, CA, USA*

<sup>2</sup>*Department of Chemical Engineering, Massachusetts Institute of Technology, Cambridge, MA, USA*

**Abstract:** This chapter focuses on micro devices aimed at rapid analysis of cells and subcellular components, specifically organelles. These devices take advantage of microfabrication techniques to create environment suitable for biomechanical and biochemical stimulation of cells, to break cell membranes to extract intracellular materials, and to separate or concentrate organelles and proteins of interest. These procedures require much smaller amounts of samples, reagents, and process time than needed in their macroscopic counterparts. Moreover, they demonstrate operational advantages, such as lower voltages, less heating, and no significant gas formation in electrolysis.

**Key words:** cell culture, subcellular separation, organelles, modeling

## 1. INTRODUCTION

Biological experiments often require extensive sample preparation. Many of the labor-intensive and time-consuming procedures can benefit from microfabricated devices that ultimately could be combined in an integrated, on-chip analysis system. Towards this goal, we envision components that are individually capable of handling biological samples at different stages of the preparation and analysis. For example, in the context of studying apoptosis (programmed cell death), it is important to use biologically relevant samples, i.e., cells that are cultured under normal bench-scale experimental conditions and biochemical treatment, and to be able to preserve and analyze the biochemical nature of the cells and subcellular materials (organelles in particular). One approach is to build

devices that are capable of (1) culturing cells for short and long terms, (2) lysing cells and releasing subcellular materials, (3) separating and isolating of subcellular materials, and (4) facilitating the identification of biochemical species of importance. This requires combination of careful analysis of the physical and chemical processes involved as well as intelligent design and microfabrication techniques. This chapter presents a few device case studies towards the goal of an integrated system for intracellular analysis on chip. Section 2 reviews a method for short and long term culture of cells and assessing cell adhesion. Section 3 focuses on a miniaturized isoelectric focusing method for organelle separation and characterization. Cell lysis in miniaturized systems, which has been accomplished by electroporation [1] among other techniques, is covered elsewhere in this volume. We conclude by suggesting a platform for integration of analysis techniques to gain insight into complex biological systems as well as development of therapeutic strategies.

## 2. CELL-CULTURE ON CHIP

### 2.1 Background and Motivation of Miniaturization

Many mammalian cells are adherent. In *in vitro* experiments, cells are cultured and stimulated either biochemically or physically. Therefore, one of the upstream processes is cell culture and stimulation on-chip. It is also desirable to use these devices to characterize cell adhesion under a variety of conditions since adhesive interactions between cells and their physical environments are central to biological activities, e.g., proliferation and migration.

A simple channel geometry provides a first order estimate of the forces applied to the adherent cells at the wall. The small dimensions of the micron-sized channels ensure laminar flow even at high linear fluid velocities because of the small Reynolds number ( $Re = u h \rho / \mu$ ) [2]. High velocities allow the generation of very large shear stresses, which is an important feature since many existing adhesion assays are limited by the practical range of applied forces achievable. The microfluidic devices also only require small amount of reagents (e.g., active biomaterials and soluble factors) and shear fluids. Typical volumes of devices described in this chapter are on the order of 1  $\mu$ l. Moreover, the devices can be operated in parallel for high-throughput experimentation.

## 2.2 Short Term Adhesion Assay Device

The design of the microfluidic cell adhesion device is motivated by the following experimental objectives: systematic variation of ligand-receptor interactions and shear stress; ability to perform short-term (< 30 min to 1 hr) as well as long-term (> 12 hr) adhesion studies; and eventual implementation of the techniques in high-throughput assays.

The device design is guided by both analytical and numerical solutions of the laminar flow problems in confined channels. Figure 11-1 compares the different values of shear stress as a function of flow rate that were derived from the Poiseuille assumption, and the 3-D analytical solutions for rectangular channel flow.

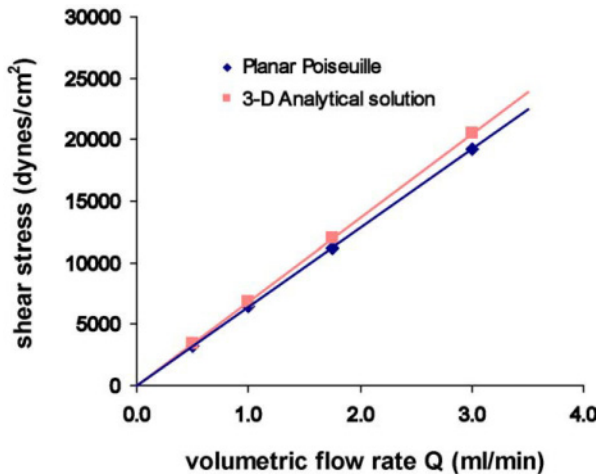


Figure 11-1. Wall shear stress as a function of flow rate from planar Poiseuille model and the 3-D analytical model.

The 3-D simulations further reveal that more than 90% of the width of the channel experiences a uniform shear stress distribution, consistent with the general observation that the wall effect persists within one height from the sidewall [3]. Therefore, in the designs with high aspect ratios (width/height), most of the cells are subject to a uniform shear stress. Fully developed flow under experimental conditions is another related design requirement. The entrance length, i.e., the length it takes for the flow to become fully developed, is a function of the Reynolds number ( $Re$ ); the larger  $Re$ , the longer the entrance region. For our experimental conditions,  $Re$  spanned from unity to a few hundred, depending on the flow rate. Estimates based on correlations [3] as well as the abovementioned numerical calculation of flow in flat channels indicate that the entrance length is below 1 mm, which is small compared to the length of the channel (10-20 mm).

Figure 11-2 (left panel) shows a multi-sample device in which four channels can accommodate either different substratum coating or different cell types. The devices are realized in poly(dimethylsiloxane) (PDMS) and bonded to microscope slides. When different substratum materials are used (e.g. extracellular matrix proteins of different types and concentrations), the materials are delivered from the four channel inlets while cells and shear fluids are introduced from the common single inlet.

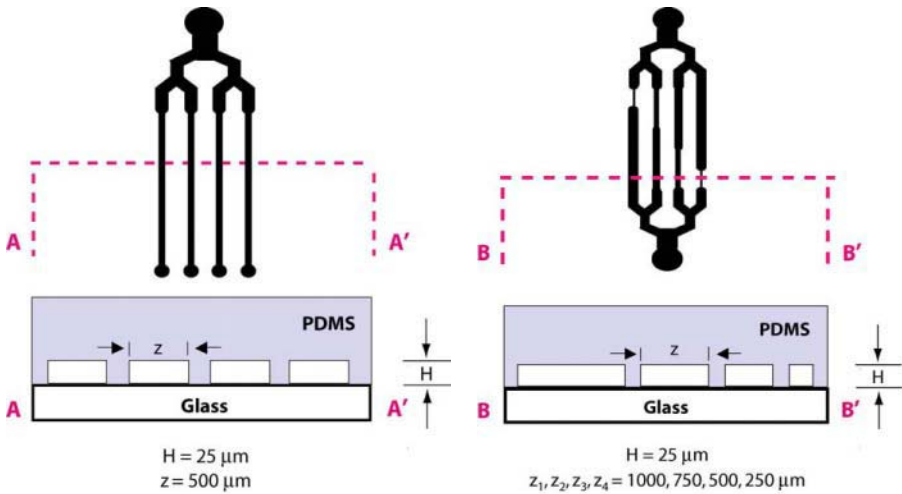


Figure 11-2. Left panel: Layout of the multi-sample device. Right panel: Layout of the multi-shear device.

Figure 11-2 (right panel) shows the layout of the multi-shear devices in which different shear forces can be created simultaneously on the same chip platform. In this case, the coating material, the cell suspensions, and the shearing fluid are common reagents, and therefore, only one inlet and one outlet are necessary. The widths of the channels were determined using the analytical models, and the lengths of the channels were compensated to ensure equal pressure drop. The design purpose here is to create multiple shear stresses to examine the time-dependent behavior of cell adhesion under shear stress.

### 2.3 Long Term Assay Devices

Many biological experiments require either cells that have been well-attached or long-term studies of adherent cells or biomaterials. In these situations, it is desirable to create a platform where cell viability can be maintained, and other soluble factors or reagents can be delivered uniformly

to the cells. This section introduces the design of such long-term assay devices.

We first consider nutrient and exogenous reagent delivery. Unlike the short-term assays, nutrient depletion becomes a critical issue in experiments that require long-term cell culture. A two-layer device is designed to provide continuous medium perfusion through a bifurcated side-channel network (Figure 11-3). Such a flow distribution scheme minimizes the subsequent shear stress experienced by the cells during delivery and ensures uniform delivery along the main channel. The shear stress experienced by the cells during is physiologically insignificant ( $< 0.5$  dynes/cm<sup>2</sup>).

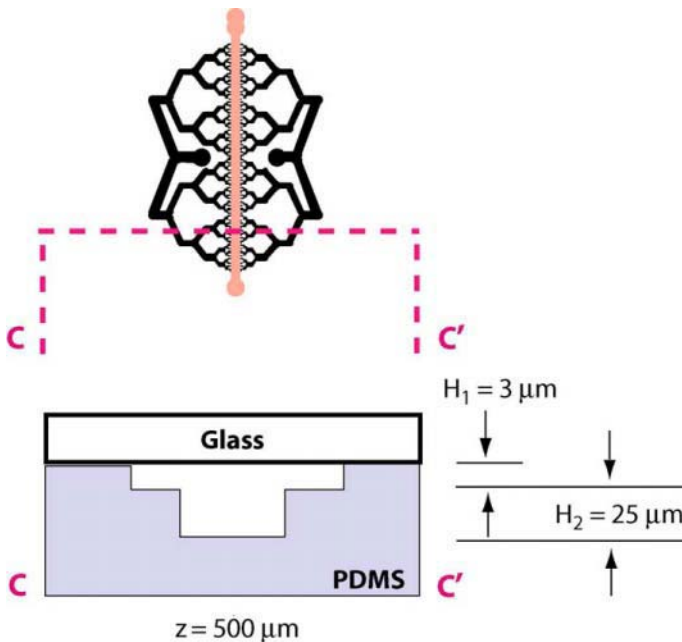


Figure 11-3. Layout of the two-layered perfusion devices for long-term cell adhesion studies. The (black) bifurcated channels are the perfusion channels, and the (orange) center channel is the shear channel.

Time scale for diffusion provides a conservative estimate of that for material delivery and exchange because fluid convection will enhance the mass transfer even further. Diffusive mass transfer from the top of the channel to the bottom ( $\sim 25$   $\mu\text{m}$ ) occurs in  $\sim 1$ -10 sec compared to the average fluid residence time in the micro channel of  $\sim 1$  min. In the device, the perfusion mass-transfer time scale is therefore sufficient for satisfactory material exchange between the cells and the fresh medium. Other additional

advantages of the two-layered design include: (1) the small thickness (3  $\mu\text{m}$ ) of the perfusion network prevents the cells from entering the side channels, thereby minimizing flow obstruction arising from cells and debris; (2) the flow provides adequate gas exchange and minimizes the probability of bubble formation; (3) the perfusion network can also be used to deliver exogenous reagents such as cell stimulants, inhibitors, or toxins for different studies.

The microfluidic devices were fabricated using PDMS rapid prototyping technique [4]. The goal of this device development is to provide biological researchers a simple-to-use platform for such adhesion assays, specifically, to develop a single-use device that is easy to assemble and handle in any lab conditions. Therefore, we chose the replication technique that does not require clean-room conditions and expensive operations.

## 2.4 Cell Culturing and Adhesion Assays

As an example, we used the fibroblast cell line WT NR6, a 3T3 variant that lacks endogenous epidermal growth factor receptor (EGFR) but that expresses stably-transfected human EGFR [5, 6]. The devices were sterilized with ethanol and the channels coated with human plasma fibronectin of various concentrations followed by Bovine Serum Albumin (BSA) to block nonspecific adsorptions. Video microscopy was used to track cells during experiments. The fraction of adherent cells was determined for each channel as the number of cells remaining adherent at a given time divided by the initial number of cells when no flow was applied. In the long-term assays, cells were sustained for growth overnight by medium delivered using a syringe pump. Attached cells were challenged with EGF and their adhesion was measured in these micro shear devices.

### 2.4.1 Cell Adhesion in Multi-Channel Short Term Device

In the multi-substrate microdevices, the measured adhesion difference can be attributed solely to systematic variations in ligand-receptor interactions. By introducing step increases in the shearing buffer flow rate at discrete time intervals, shear stress was increased from 0 to 1,600 dynes/cm<sup>2</sup> (based on Poiseuille calculation) with time throughout the assay to sample increasing levels of shear-force response. Figure 11-4 demonstrates that cell adhesion strength depends on the fibronectin surface density. The range of stress (0 - 1,600 dynes/cm<sup>2</sup>) is well within the capability of the devices. The case study further demonstrates that microfluidic adhesion devices can be used to probe cell adhesive response to ECM ligand concentration in a high-throughput format.

There are many instances where the measurement of interest is the dynamic biophysical response of cells to different external forces. The multi-shear device achieves built-in variation in shear stress across the channels by giving each channel a different width while maintaining identical pressure drop by compensating with the length of the channels. For example, when channel width is narrowed from 1000  $\mu\text{m}$  to 750  $\mu\text{m}$  and to 500  $\mu\text{m}$ , the length is shortened accordingly, and a 1.5-fold and 2-fold increase in shear stress, respectively, is effectively introduced. Shear stress values as high as 4000  $\text{dyne}/\text{cm}^2$  were achieved in this micro device. Different cell adhesion profiles were obtained in the high adhesion regime (10  $\mu\text{g}/\text{ml}$  of fibronectin), as illustrated in Figure 11-5. Thus, the multi-shear device provides a systematic approach to varying shear stress and determining the force level that is most relevant for the adhesion measurement of a cell population of interest. Modification of this device configuration could potentially provide a platform for studying kinetics and mechanisms of cell detachment from specific substrates.

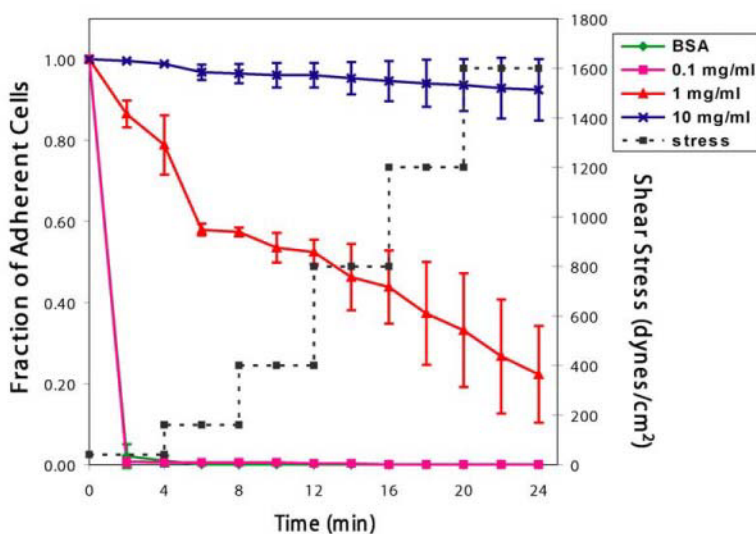


Figure 11-4. Cell adhesion assay in multi-sample device where the substrate is coated with fibronectin of various concentrations.

## 2.4.2 Long Term Shear Assays – Nutrient and Reagent Delivery

Long-term cell adhesion is rarely quantified, in part because tremendous forces are required to detach well-adherent cells such as fibroblasts. Long-term incubation in micro devices is a challenge. A typical microfluidic

channel holds a total volume on the order of a few microliters, which makes nutrient delivery and medium exchange critical in maintaining long-term cell viability. As illustrated in Figure 11.6, when cells were incubated in the long-term device for 12 hours without perfusion, many of the cells rounded up or had fragmented cell membranes, indicative of unhealthy or dying cells. In contrast, when fresh assay medium was delivered at a small flow rate, cells continued to spread and retained an appearance that is similar to those cultured under macroscopic conditions. The presence of flow also helped to suppress nucleation of gas bubbles, which otherwise can be a problem in micro devices because of the large surface area and accumulation of cellular debris.

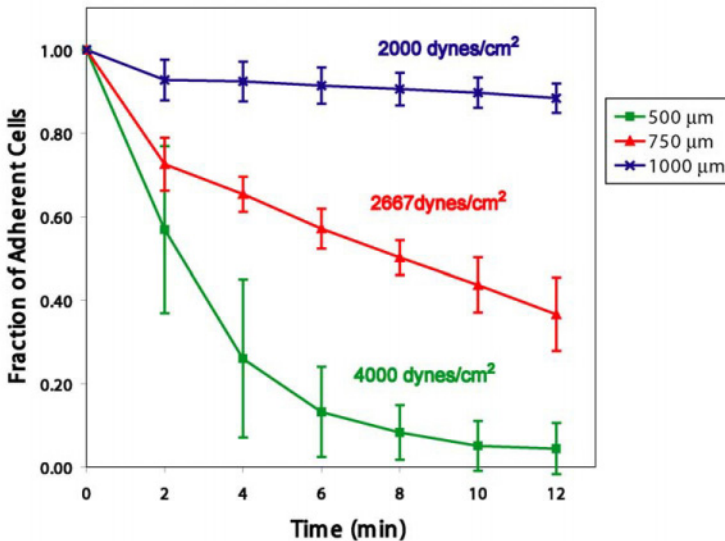


Figure 11-5. Cell adhesion assays in multi-shear device where different shear stresses are applied to adherent cells.

### 2.4.3 Long Term Shear Assays – Nutrient and Reagent Delivery

Long-term cell adhesion is rarely quantified, in part because tremendous forces are required to detach well-adherent cells such as fibroblasts. Long-term incubation in micro devices is a challenge. A typical microfluidic channel holds a total volume on the order of a few microliters, which makes nutrient delivery and medium exchange critical in maintaining long-term cell viability. As illustrated in Figure 11-6, when cells were incubated in the long-term device for 12 hours without perfusion, many of the cells rounded up or had fragmented cell membranes, indicative of unhealthy or dying cells.

In contrast, when fresh assay medium was delivered at a small flow rate, cells continued to spread and retained an appearance that is similar to those cultured under macroscopic conditions. The presence of flow also helped to suppress nucleation of gas bubbles, which otherwise can be a problem in micro devices because of the large surface area and accumulation of cellular debris.

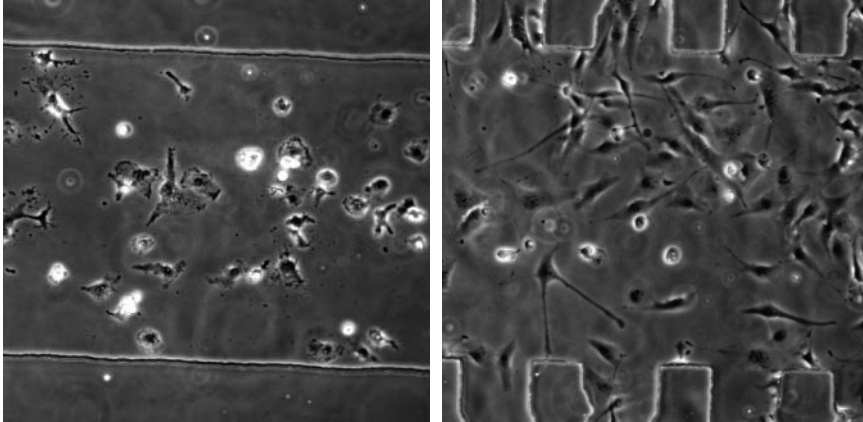


Figure 11-6. Comparison between cells (on 10  $\mu\text{g/ml}$  of fibronectin) that were incubated with (right) and without (left) medium perfusion at 37  $^{\circ}\text{C}$  for 12 hrs.

Cell adhesion is regulated not only through adhesion to substratum ligands, but also by soluble biochemicals and peptides. For example, EGF has an established role in disassembly of focal adhesions, thereby reducing cell adhesion and in many cases enhancing cell motility [7-9]. Using the perfusion device, WT NR6 fibroblasts were first serum-starved. The perfusion network then uniformly delivered EGF to sample channels. After treatment, the adhesion assay was performed to assess cell response. The weakening effect of EGF on cell adhesion is demonstrated in Figure 11-7. It was possible to remove fully spread fibroblasts at the end of the assay by applying  $\sim 6000$  dynes/cm<sup>2</sup>, using a flow rate that is well within the technical limit of the system. This threshold of detachment force is comparable to macro scale experiments [10], and it is in agreement with theoretical calculations [11].

### 3. SUBCELLULAR FRACTIONATION – ORGANELLE SEPARATION

#### 3.1 Background and Motivation

The preparation of samples for biochemical analysis of subcellular protein activity often requires cell lysis, fractionation, and purification of organelles. For example, to assay cytochrome *c* translocation from the mitochondria to cytosol during type II apoptosis in mammalian cells, one must isolate the cytosolic and mitochondrial fractions [12, 13]. Similarly, to monitor the translocation of steroid hormone receptors from cytoplasm to the nucleus, a nuclear fraction must be prepared. The speed of the separation is particularly important in studies of early biochemical events after stimulations of the cells [14]; for example, many caspases can be activated early on in apoptosis.

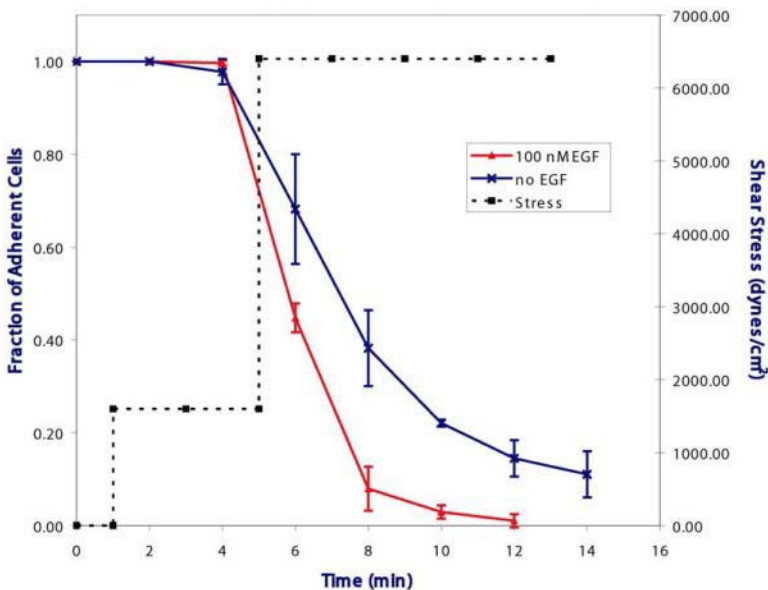


Figure 11-7. Microfluidic shear assay on effect of EGF on cell adhesion.

Current methods of organelle separation, such as density-gradient centrifugation, immunoisolation, or electromigration analysis, typically require many labor-intensive steps, and they are not suitable for small-sample analysis. Density gradient centrifugation relies on different densities

of organelles [13]. Typically, the density gradient is set up by centrifugation in the presence of sugar (e.g. sucrose and manitol). Different centrifugation forces yield supernatant and pellet fractions containing different organelles. Multiple-organelle separation or single-organelle isolation therefore requires multiple/repeated spin steps in different buffers to achieve the desired separation. Centrifugation is generally robust and readily scalable for large *amounts* of samples for preparative purposes, but the manual operations (spin and pipetting) are time-consuming. Moreover, the complexity of manipulations makes it difficult to handle very small *amounts* and large *number* of samples for analytical purposes.

Immunoisolation makes use of the specificity of the interactions between organelle specific proteins and antibodies [13]. Typically antibodies against organelle surface proteins are immobilized on solid supports, which are packed into columns. The cell lysates are flow through the columns where the specific organelles are captured onto the solid supports. In subsequent steps, the organelles are eluted from the column by changing pH conditions. Because it relies on specific protein-protein recognitions, immunoisolation technique is highly specific; however, it is also relatively expensive [13]. Similar to centrifugation techniques, it requires multi-step sample handling. Both of these methods have the disadvantages of being time-consuming and having sample-loss during handling.

In contrast, electromigration separation techniques for separation of cells, membranes, proteins, or other biological particles are usually single-step procedures. Variations of electromigration separations, including free flow electrophoresis (FFE), high-resolution density-gradient electrophoresis, and immune free flow electrophoresis, utilize the different charges (sometimes in combination with other properties, such as density and size) of biological particles and macromolecules to achieve the separation. However, these methods require substantial voltages and power input. As a result, Joule heating in these devices can sometimes be substantial. In order to maintain the resolution and quality of the separation, one usually has to provide adequate cooling using water jackets. Furthermore, these techniques still consume a considerable amount of sample, as well as time, usually on the order of a couple of hours. The reason is that the analytes have to traverse distances on the order of a few centimeters. The mobilities of the analytes are fixed by their surface properties and the local pH conditions, and the time scale for the electromigration greatly depends on the electric field strength applied to the system. To speed up such separation steps, larger voltages can be used. However, practical complications (e.g. electrolysis of water and heating effects) could limit the lower bound of the time scale of such processes. Therefore, in many systems, gels or other stabilizing media

are used to reduce the secondary flow at the expense of having extra steps and reduced flexibilities.

Systems biology studies require large data sets on multiple-protein profiling of many samples. Consequently, parallel and automated organelle separation is desirable, as are methods allowing the use of small populations of cells. Microfluidic systems, such as DNA separation chips [15-17],  $\mu$ FACS [18], micro diffusion sensors [19-21], , and smart valves [22-24], have demonstrated superior performance compared to their macroscopic counterparts. In choosing a separation scheme, we considered the physical/biochemical properties distinguishing the organelles and practicality of the procedure in small scale. The organelles have different shapes and diverse size distribution; however, these characteristics are rarely sufficient to distinguish many organelles from each other. For example, mitochondria can be as large as 1  $\mu\text{m}$  and as small as 100 nm with a spherical or ellipsoidal shape, while the endoplasmic reticulum (ER) is membranous and does not assume a defined shape. Therefore, using size exclusive filters to separate these two organelles is not practical. On the other hand, one can take advantage of the biochemical and charge characteristics of the organelles. Although electrophoretic methods are not as specific as immuno-affinity separation methods, it is a single step procedure that achieves a rough separation.

As a case study, we illustrate a microfluidic device for separating organelles by isoelectric focusing (IEF). This device has several advantages over conventional macroscopic systems. First, the speed for separation is improved by orders of magnitude since the distance that analytes travel is greatly reduced while the system maintains the same driving force -- fixed field strength. Second, the same field strength is achieved by applying only a small voltage, usually of three orders of magnitude reduction. Consequently, the Joule heating is negligible ( $\sim 10^6$  less power consumption than in macro systems) and the separation resolution is maintained without the introduction of external cooling devices. The volume of the microfabricated devices can be as small as sub-microliter, most suitable for parallel analysis of multiple samples. Lastly, the microfluidic IEF device can be interfaced with other microfluidic devices for systematic probing of cellular activities and subcellular biochemistry.

### 3.2 Isoelectric Focusing

In electromigrational separation methods, the presence of the surface charges on the analytes gives rise to different mobilities under the influence of the electric field. In protein IEF[25-27], a protein molecule is mobilized under the influence of an external electric field within a pH gradient (Figure

11-8). The pH gradient is established and maintained through water electrolysis at the electrodes with an externally applied voltage and supplied current (creating protons and hydroxide ions). Ampholyte buffer species are also added to the separation medium to control the formation and stabilization of the pH gradient.

Organelle surfaces contain many proteins and other amphoteric molecules, such as glycoproteins [28]. These surface molecules with their individual pI's would give rise to the apparent pI of the organelles. The time required to focus particles and organelles can be long, due to the much larger drag force on particles compared to that on protein molecules. The speed at which organelles migrate is proportional to their electrophoretic mobility, a function of their size and charge, and to the fixed electric field strength.

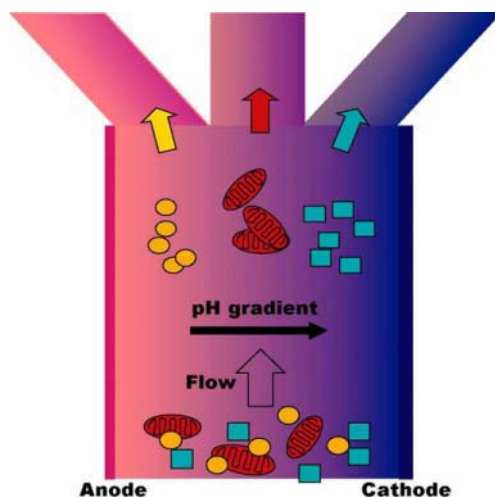


Figure 11-8. The separation principles of isoelectric focusing.

### 3.3 Understanding IEF Performance in Micro Devices

We use scaling arguments as well as numerical models to understand the relative time scales of different phenomena (e.g. the pH gradient formation and electromigration of species) in relations to geometry, operating voltages, and current densities. The focusing effect is dependent on three separate physical effects: convective transport by the carrying fluid, the electrophoretic transport driven by the applied electric field, and diffusion from Brownian motion. The relative importance of these factors are reflected in two Peclet numbers:  $Pe = UL_x^2/DL_z$  with the usual definition of convection relative to diffusion, and  $Pe_e = \mu EL_x/D$  with electrophoresis relative to diffusion.

Microfluidic systems are designed so that the time scales for electrophoretic focusing and the time scale for convective transport are on the same order of magnitude, i.e., the two Peclet numbers are roughly equal. For example typical numbers are: linear velocity ( $U$ )  $\sim 100 \mu\text{m/s}$ , length scale in the length ( $z$ ) direction ( $L_z$ )  $\sim 10 \text{ mm}$ , length scale in the cross flow direction ( $x$ ) direction ( $L_x$ )  $\sim 1 \text{ mm}$ , particle diffusivity  $D \sim 10^{-12} \text{ m}^2/\text{s}$ , mobility of mitochondria  $\sim 1 (\mu\text{m/s})/(\text{V/cm})$ , and electric field strength  $\sim 1 \text{ V/mm}$ . In this case, the convective and electrophoretic Peclet numbers are both  $\sim 10^4$ . Although a useful starting point, the scaling analysis is limited by the highly nonlinear concentration profile of the organelles caused by the non-linearity of their surface charges. Therefore, simulations are needed to examine details of diffusion and convective/electrophoretic transport.

The first goal of the model is to establish the time required for pH gradient to be set up in a micro device. To model pH gradient formation, the model has to include electrolysis of water at the electrode, the mobilization of charged acid/base species, and acid/base reactions in the bulk. The mobility of small ions and non-amphoteric molecules were assumed to be constants while in reality the mobility may vary slightly depending on the local ionic strength and other screening effects.

As the next step, we formulate a model for BSA focusing in a pre-established pH gradient and estimate the focusing time for a protein. This one-dimensional (1D) pseudo-time-dependent model also provides an estimate of focusing of amphoteric molecules in the absence of detailed information on mobility and charge characteristics of the ampholytes (low molecular weight polyamino-polycarboxylic acids) in commercial, proprietary ampholyte solutions.

Figure 11-9 shows the resulting simulations of BSA focusing. The time in the simulation corresponds to the length (or the flow) direction of the device: the earlier time represents the concentration profile closer to the inlet, and the later time the concentration profile closer to the exit. The molecules are initially well distributed ( $t = 0 \text{ sec}$ ), and gradually move towards the pI (subsequent time traces). The final concentration profile does not change with time (with downstream position) when a balance between electrophoresis and diffusion is achieved. Thus, longer focusing does not improve the resolution of the separation process in IEF. The time scale for focusing BSA is on the order of 20-30 seconds using a 2 V potential in a 1 mm wide micro-device. In contrast, typical macro-scale IEF requires over 1 kV for at least 30 min [25]. We estimate the speed of pre-focusing, i.e., the focusing time of the ampholyte species stabilizing the pH gradient, to be  $\sim 30$  seconds.

An analogous approach is used to model mitochondria focusing in the micro-device to gain an understanding of the dynamic process and aid the

device design. The movement of mitochondria in the micro-device is governed by the electrophoretic force due to the external electric field, Brownian force, and the fluid drag force. Since mitochondria surface contains many protein species, the charge distribution and surface characteristics are complex. Consequently, lumped model based on the effective electrophoretic mobility and the diffusion of the mitochondria particles is used in the simulations. Values reported in the literature for the free flow electrophoretic mobility of mitochondria from rat kidney cells [29] are used in the present case study.

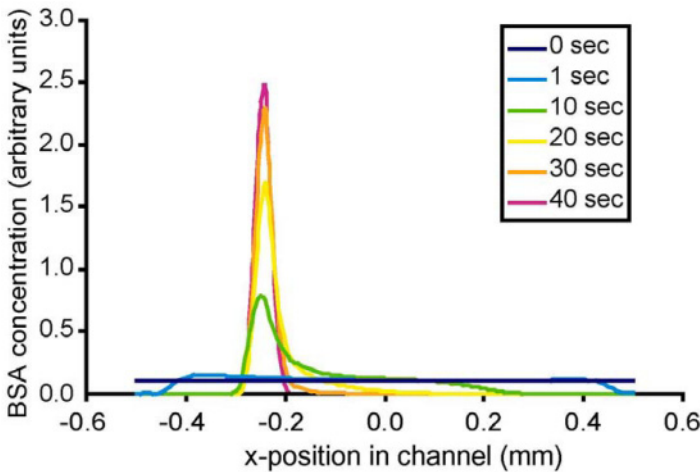


Figure 11.9. Focusing BSA: 1D Pseudo-Time-Dependent Model. See also Colour Plate Section page 356.

Figure 11-10. shows that focusing of the rat mitochondria took place in approximately 4 minutes. The evolution of the concentration profile for mitochondria is similar to that for BSA. The simulation suggests that pH prefocusing is much faster than mitochondria focusing, and may be neglected in future models. In addition, at the micro scale, Brownian diffusion appears to have a significant impact on the width of the concentration distribution. For particles, no significant “shoulder develops” in the concentration profile and the final distribution is much narrower because the diffusivity is small.

A three-dimensional (3D) model provides insight into the interplay among diffusion, velocity profile of the pressure-driven flow, and electrophoretic force on the concentration profile. In particular, it allows evaluation of the influence of the actual 3D parabolic velocity profile on the focusing speed. Additionally, it shows whether the pseudo-time-dependent 1D model is sufficient to predict the separation process. The simulations (Figure 11-11) reveal that the Brownian diffusion of the particles is not

significant when the local concentration of mitochondria is low (e.g. near the inlet of the channel), but becomes important when the mitochondria are focused. Similar to the 1D pseudo-time-dependent model, Brownian diffusion balanced the electrical force at steady state, and together they determined the concentration distribution of the focused stream. The flow rate is chosen so that the mitochondrial concentration reaches a steady profile at the exit of the flow channel, corresponding to a residence time of  $\sim 4$  min, in good agreement with the 1D model. This implies that the parabolic velocity profile and back diffusion have no significant influence on the evolution of the concentration profile.

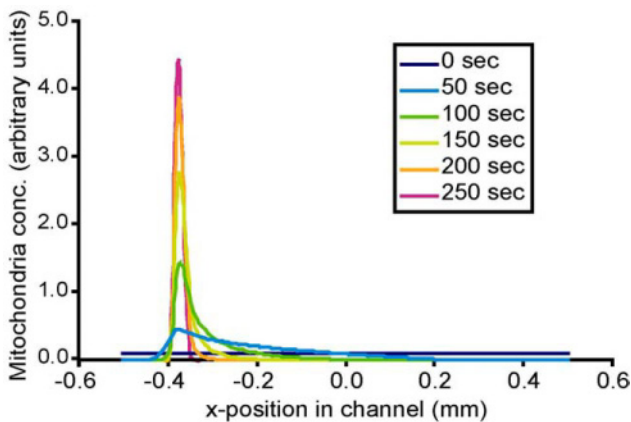


Figure 11-10. Focusing Mitochondria: 1D Pseudo-Time-Dependent Model

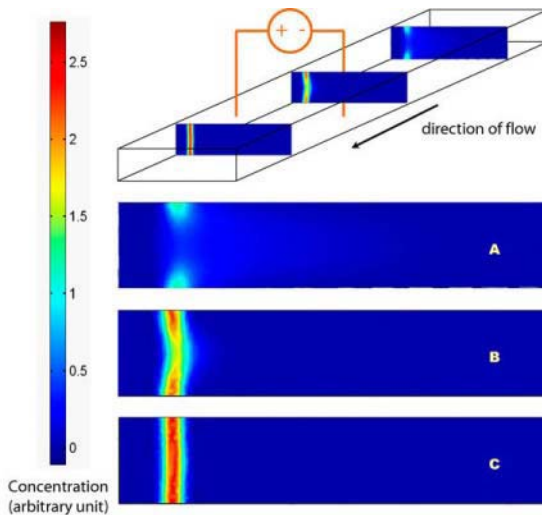


Figure 11-11. Three-dimensional model of mitochondrial isoelectric focusing in microfluidic channels. See also Colour Plate Section page 357.

### 3.4 Device Design and Fabrication

The device layout (Figure 11-12) is similar to macroscopic field flow fractionation unit: the flow is in the length direction ( $z$ ) direction, the electric field in the cross flow direction ( $x$ ) direction, and the aspect ratio is large, i.e., the depth ( $y$ ) is small. In the present design, the channel is 18 mm long, 1 mm wide and 50  $\mu\text{m}$  deep. Four channels (250  $\mu\text{m}$  wide) are included in the prototype device as a means for collecting separate fractions of the focused fluid. The bottom of the device is composed of glass, with metal (gold and titanium) thin film electrodes. The channel is formed in photo-patternable epoxy (SU-8), which easily allows for design modifications.

To implement the design, devices were fabricated using a combination of photolithography, electron-beam metal deposition, and liquid-phase electro-deposition. To achieve a uniform electric field in the separation portion of the devices, we electroplated vertical electrodes on the sidewalls of the channel instead of using planar thin-film electrodes. These electrodes also lasted longer in corroding environments (in the presence of an electric field and chloride ions), ensuring reusability.

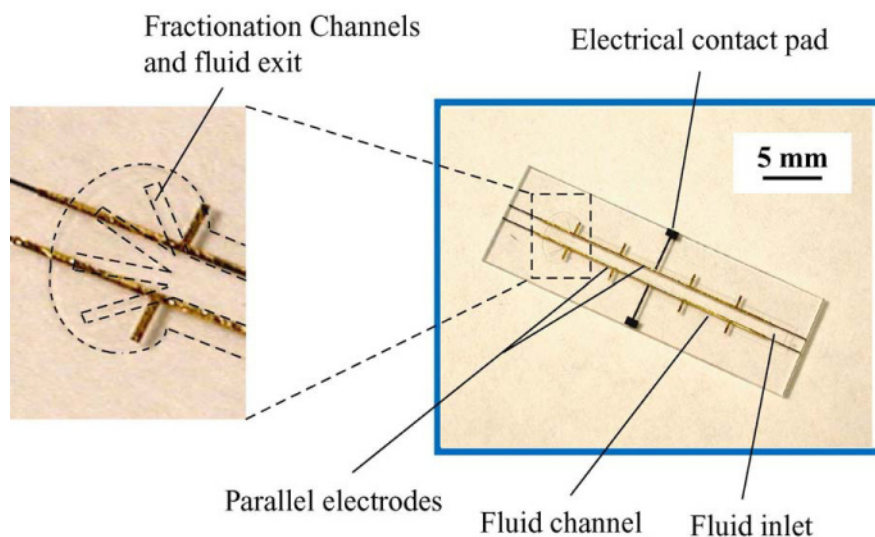


Figure 11-12. Microfabricated IEF device with fraction collection channels. See also Colour Plate Section page 357.

### 3.5 $\mu$ IEF of Mitochondria

Human HT-29 cells, HeLa cells, NR6WT murine fibroblasts were cultured using standard protocols. For the experiment using apoptotic cells, HeLa cells were treated with Tumor Necrosis Factor and cycloheximide, and

the floating cells were collected. The mitochondria were labeled in live cells with MitoTracker™ Green or Red or JC-1 (Molecular Probes Inc.). To prepare the cell lysate and mitochondria fractions, the cells were suspended in buffers, swollen, and sheared through a needle. The nuclei were labeled using propidium iodide. In the experiments, either cell lysate or a crude mitochondrial fraction (prepared by density gradient centrifugation) was used. To label peroxisomes with GFP, a construct driving the expression of EGFP with a peroxisome targeting signal was prepared, and HeLa cells were transiently transfected with this construct.

A microfabricated device was mounted on an inverted fluorescence microscope with a digital camera. Before each experiment, the device was first flushed with bleach, water, and buffer. BSA solution was flushed through the device, and incubated to passivate the device walls. For IEF experiments, ampholine buffer solution was used.

### 3.5.1 $\mu$ IEF of Roughly Purified Mitochondrial Fraction

The following case study illustrates that mitochondria exhibit amphoteric surface characteristics under experimental IEF conditions, and can be focused in the microfabricated device. A sample with MitoTracker-labeled HT-29 cell lysate enriched in mitochondria by differential centrifugation was delivered through plastic tubing using pressure-driven flow. At a  $\sim 2$  V applied potential, the mitochondria are focused in the channel under flow condition (Figure 11-13). When the mitochondria fraction is first introduced into the device, the mitochondria are present throughout the channel width (Figure 11-13 top). As they flow through the channel, the pH gradient develops and focusing of mitochondria starts to take place (Figure 11-13 middle). A residence time of  $\sim 6$  min produces a steady state of focused mitochondria near the exit of the channel (Figure 11-13 bottom). These experimental results match the evolution in the concentration profile obtained from numerical simulations using electromobility data from rat kidney mitochondria. The slight difference in the predicted and experimental focusing times may be attributed to physiological differences between rat and human mitochondria, differences in the size distributions of the particles, and in the buffer compositions (e.g. ionic strength). Compared to conventional methods of organelle preparation, the micro-scale IEF is orders of magnitude faster.

As an example of using the flow splitter at the end of the IEF channel to collect different fractions, Figure 11-14 demonstrates fluorescently labeled cells, cellular fragments, and nuclei being directed into the corresponding channels. Thus, it would be possible to collect or redirect bands of separated

organelles or macromolecules of interest for subsequent analysis or further refinement of the separation.

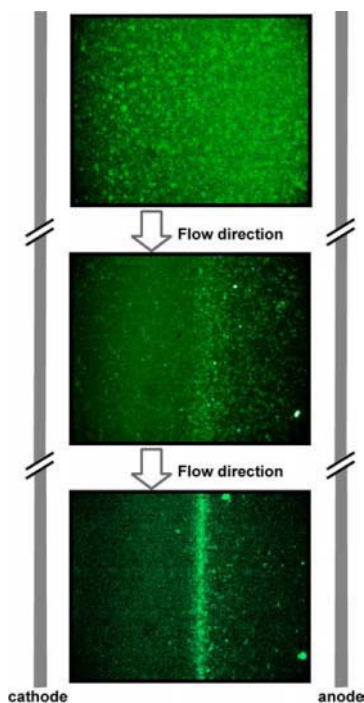


Figure 11-13. Focusing pre-purified mitochondria from HT-29 cell lysate.

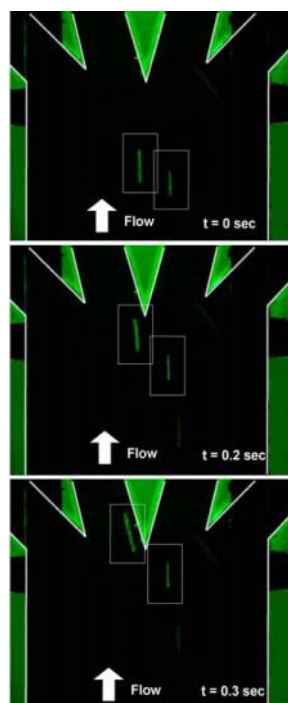


Figure 11-14. Splitting flows in the flow fractionation device.

### 3.5.2 $\mu$ IEF of Mitochondria from Cell Lysate

The next example (Figure 11-15) illustrates separation directly from cell lysate without prefractionation. Intact cells (visible because they contain labeled mitochondria) migrate towards the anode because of the acidic character of the plasma membrane. In the range of pH used in this experiment (pH 3-10), the cell membrane always carried negative charges. This demonstration of focusing of mitochondria in the presence of membrane debris, cytosolic materials, other organelles, and intact cells, shows promise for using this module as a separation component directly downstream from a cell lysis unit.

### 3.5.3 Separation of Subpopulations of Mitochondria

It is well known that mitochondria lose their transmembrane potential during type II apoptosis associated with cytochrome *c* release. The subpopulations of mitochondria that maintain the intact transmembrane potential and that lose the potential could possess different surface properties that would allow the separation in the  $\mu$ IEF devices. To test this hypothesis, mitochondria from HeLa cells is stained with the membrane-potential-sensitive dye JC-1 (Molecular Probes, Inc.). For physiologically normal mitochondria retaining transmembrane potential, JC-1 accumulates in the membrane as the red-fluorescent “J-aggregates”, while the monomer at low concentration at low membrane potential exhibits green fluorescence. Therefore, using ratiometric measurements, it is possible (1) to visualize the two populations of mitochondria; (2) to determine whether the mitochondria still maintain their transmembrane potential during the  $\mu$ IEF preparation.

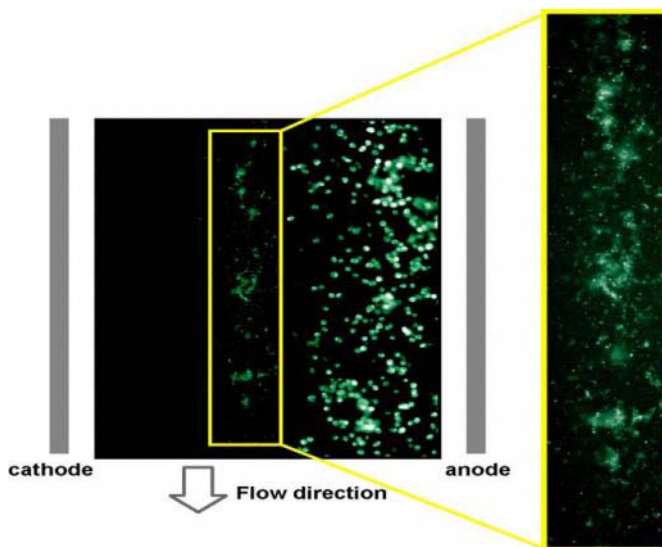
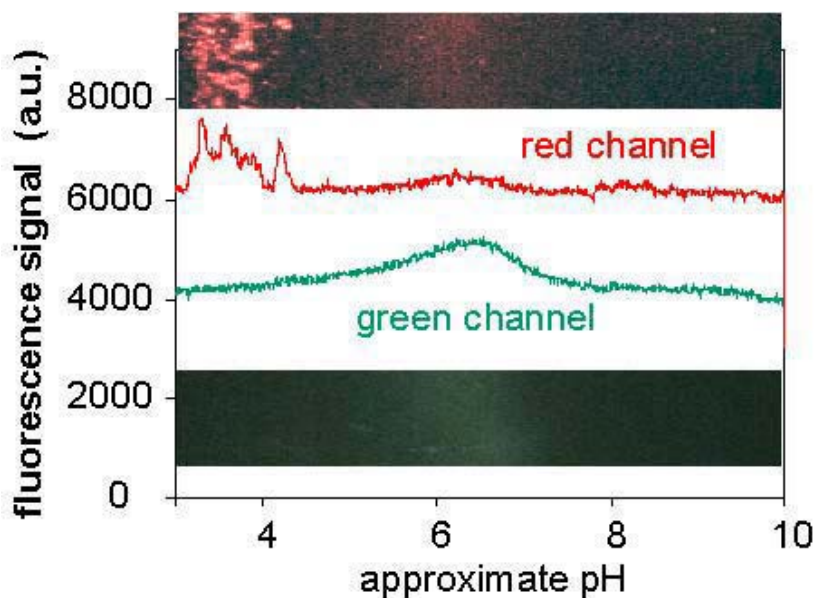


Figure 11-15. Focusing mitochondria from direct HT-29 lysate

Close to the exit of the  $\mu$ IEF device, there are two populations of mitochondria (Figure 11-16) – red and green fluorescent populations. The mitochondria that have lost membrane potential are expected to be less charged, i.e., more neutral. Indeed, the majority of the mitochondria in the red channel have a more acidic pI, whereas the mitochondria in the green channel have a pI close to neutral. These observations indicate that the separation process exerts minimal damage to the mitochondria.

### 3.5.4 Extending IEF to Other Organelles

Experiments with crude lysate from NR6wt (murine fibroblasts) cells with labeled mitochondria and nuclei demonstrate the technique's ability to separate different organelles and extend to yet another cell type. The mitochondria from NR6wt cell also form a tightly focused band (Figure 11-17). (The slightly different appearance of mitochondria in different figures is caused by different experimental and microscopy conditions). The nuclei migrate to one side of the devices and they are not focused as efficiently as mitochondria are, probably due to their larger size and possibly non-uniform pI. Nonetheless, the mitochondria fraction is free of nuclear contamination by fluorescence microscopy. It is possible that optimization of the microIEF condition (e.g. pH range, residence time, or buffer conditions) can lead to the better focus of nuclei.



*Figure 11-16.* Separations of two subpopulations of mitochondria: (a) image in the red channel showing mitochondria with normal membrane potential; (b) image in the green channel showing mitochondria that have lost membrane potential.

Finally, we consider the separation of mitochondria and peroxisomes by using HeLa cells labeled with MitoTracker-Red and transiently transfected with GFP carrying a peroxisome localization signal. Both the peroxisomes and the mitochondria are focused and concentrate, but they co-migrated in the electric field (Figure 11-18). In this case orthogonal methods, such as

affinity-based or size-dependent separation, would be used in tandem to separate the two organelle populations. The need for using multiple separation techniques to achieve effective sorting of proteins is well known and it is not surprising that similar conditions would apply to organelles. Affinity based methods have already been demonstrated in microfluidics [30, 31] and could readily be extended to organelle sorting.

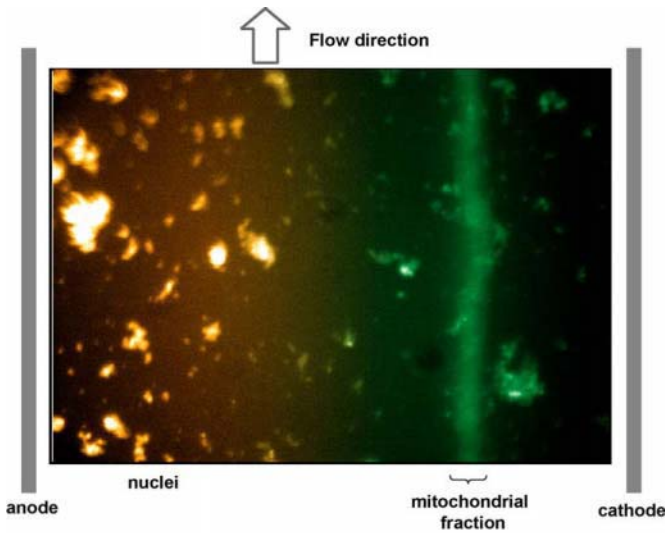


Figure 11-17. Separating nuclei from mitochondria in NR6wt cell lysate. See also Colour Plate Section page 358.

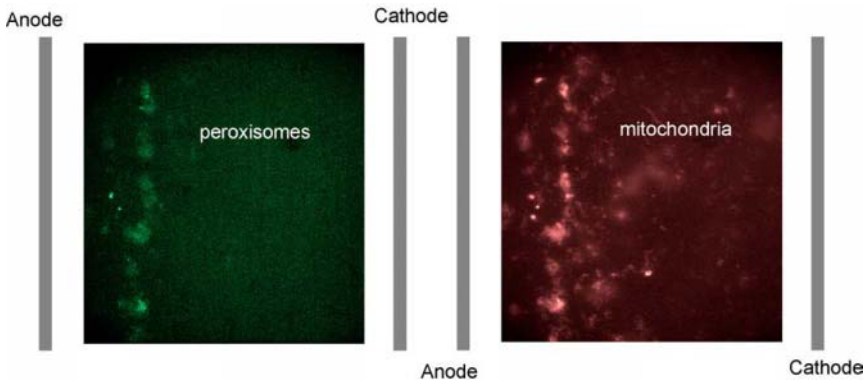


Figure 11-18. Enrichment of peroxisomes and mitochondria from HeLa cell lysate. Contrast was enhanced individually for the figures. See also Colour Plate Section page 358.

### 3.6 Discussion

Free flow separation is advantageous in part by not requiring the use of gels, which simplifies the procedure and reduce the chance of clogging. However, organelle separation in free flow is difficult at large scale. The heating of the medium resulting from the required high electrical fields can cause organelle damage and lead to density gradient-driven convections that destroy the resolution of the separation. Usually a cooling system has to be used to alleviate these problems. The voltage and resulting current used in our experiments are  $\sim 1,000$  fold less than what macro-scale devices require. Consequently, the power consumed in the micro-device is  $10^6$  times smaller. Moreover, the large surface to volume ratio of micro-devices enhances heat transfer. For example, calculations show that the temperature rise in the micro-device device is less than  $0.001$  °C without active cooling.

Another important advantage of the miniaturized device is the reduction of the time scale of the separation by shrinking the dimension of the device ( $t \sim (L/\mu E)$ ). The separation experiments are still conducted at large Peclet numbers (both  $Pe$  and  $Pe_e \sim 10^3 - 10^4$ ) with no significant back-diffusion in the direction of the flow. Since the micro-device operates in continuous mode, the amount of sample processed can be varied for different experiments. It is then possible to use the device to probe a small population of cells (as few as  $\sim 2,000$  cells in our experiments) for analytical purposes, or multiple devices in parallel operating continuously could be applied for larger scale preparation.

The microIEF technique for separation of organelles is limited to organelles (or proteins) that have significantly different isoelectric points. Even if the organelles are larger and perhaps variations in pI, this technique significantly still enriches the fraction with the organelles of interest, as shown for the case of nuclei and mitochondria separation. In addition, the same device can be operated in a variety of electrophoretic separation modes.

## 4. CONCLUSIONS AND FUTURE OUTLOOK

This chapter has explored a few examples of cellular and subcellular analysis approaches on chip. Combining cell growth, stimulates, sorting, lysis, IEF separation, and protein analysis (see Figure 11-19) in one or more integrated chip scale devices would offer advantages over macroscopic devices. Process time would be shorter because of scaling effects in micro devices. Cells and organelles would be contained within a controlled environment and processed without delay. Modularity of this approach

would also allow flexible designs to accommodate the complex nature of biological systems.

The multiplicity of the functions performed on each device and the various fabrication techniques would make the integration effort nontrivial. The overall performance of the integrated device strongly depends on the reliability of the individual unit operations. Therefore, it is critical to optimize on the individual-device and assay level. Proper surface modification and assay conditions are key for such optimization. Ultimately, cellular analysis on chip will enable a network approach to solve complex biological problems. Future personalized diagnosis and prescription of treatment will also benefit from these technologies.

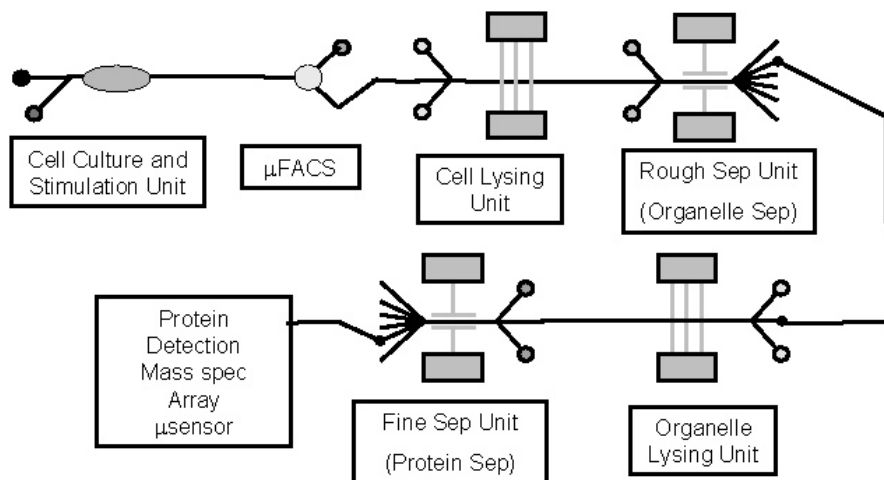


Figure 11-19. Integrated, multifunctional, and chip-based device for bioanalysis.

## ACKNOWLEDGEMENTS

We thank our collaborators Professors Martin Schmidt, Douglas Lauffenburger, Linda Griffith, Peter Sorger, Drs. Suzanne Gaudet, and Lily Koo. The work was funded by DARPA, NIH and NSF.

## REFERENCES

1. Lu, H., Schmidt, M.A., and Jensen, K.F., *A microfluidic electroporation device for controlled cell lysis*. Lab-on-a-chip, accepted.

2. Kenis, P.J.A., Ismagilov, R.F., and Whitesides, G.M., *Microfabrication inside capillaries using multiphase laminar flow patterning*. *Science*, 1999. 285(5424): 83-85.
3. Deen, W., *Analysis of Transport Phenomena*. 1998, New York: Oxford University Press.
4. Duffy, D.C., McDonald, J.C., Schueller, O.J.A., and Whitesides, G.M., *Rapid prototyping of microfluidic systems in poly(dimethylsiloxane)*. *Analytical Chemistry*, 1998. 70(23): 4974-4984.
5. Pruss, R.M. and Herschman, H.R., *Variants of 3T3 cells lacking mitogenic response to epidermal growth-factor - (receptors mitogens colchicine selection)*. *Proceedings of the National Academy of Sciences of the United States of America*, 1977. 74(9): 3918-3921.
6. Chen, P., Gupta, K., and Wells, A., *Cell-movement elicited by epidermal growth-factor receptor requires kinase and autophosphorylation but is separable from mitogenesis*. *Journal of Cell Biology*, 1994. 124(4): 547-555.
7. Xie, H., Pallero, M.A., Gupta, K., Chang, P., Ware, M.F., Witke, W., Kwiatkowski, D.J., Lauffenburger, D.A., Murphy-Ullrich, J.E., and Wells, A., *EGF receptor regulation of cell motility: EGF induces disassembly of focal adhesions independently of the motility-associated PLC gamma signaling pathway*. *Journal of Cell Science*, 1998. 111: 615-624.
8. Maheshwari, G., Wells, A., Griffith, L.G., and Lauffenburger, D.A., *Biophysical integration of effects of epidermal growth factor and fibronectin on fibroblast migration*. *Biophysical Journal*, 1999. 76(5): 2814-2823.
9. Lu, Z.M., Jiang, G.Q., Blume-Jensen, P., and Hunter, T., *Epidermal growth factor-induced tumor cell invasion and metastasis initiated by dephosphorylation and downregulation of focal adhesion kinase*. *Molecular and Cellular Biology*, 2001. 21(12): 4016-4031.
10. Garcia, A.J., Takagi, J., and Boettiger, D., *Two-stage activation for alpha(5)beta(1) integrin binding to surface-adsorbed fibronectin*. *Journal of Biological Chemistry*, 1998. 273(52): 34710-34715.
11. Olivier, L.A. and Truskey, G.A., *A Numerical-Analysis of Forces Exerted by Laminar-Flow on Spreading Cells in a Parallel-Plate Flow Chamber Assay*. *Biotechnology and Bioengineering*, 1993. 42(8): 963-973.
12. Brenner, C. and Kroemer, G., *Apoptosis - Mitochondria - the death signal integrators*. *Science*, 2000. 289(5482): 1150-1151.
13. Graham, J.M. and Rickwood, D., *Subcellular Fractionation - a Practical Approach*. *The Practical Approach Series*, ed. Rickwood, D. and Hames, B.D. Vol. 173. 1997, New York: Oxford University Press Inc.
14. Hengartner, M.O., *The biochemistry of apoptosis*. *Nature*, 2000. 407(6805): 770-776.
15. Cheng, J., Sheldon, E.L., Wu, L., Uribe, A., Gerrue, L.O., Carrino, J., Heller, M.J., and O'Connell, J.P., *Preparation and hybridization analysis of DNA/RNA from E-coli on microfabricated bioelectronic chips*. *Nature Biotechnology*, 1998. 16(6): 541-546.
16. Doyle, P.S., Bibette, J., Bancaud, A., and Viovy, J.L., *Self-assembled magnetic matrices for DNA separation chips*. *Science*, 2002. 295(5563): 2237-2237.
17. Burns, M.A., Johnson, B.N., Brahmasandra, S.N., Handique, K., Webster, J.R., Krishnan, M., Sammarco, T.S., Man, P.M., Jones, D., Heldsinger, D., Mastrangelo, C.H., and Burke, D.T., *An integrated nanoliter DNA analysis device*. *Science*, 1998. 282(5388): 484-487.
18. Fu, A.Y., Spence, C., Scherer, A., Arnold, F.H., and Quake, S.R., *A microfabricated fluorescence-activated cell sorter*. *Nature Biotechnology*, 1999. 17(11): 1109-1111.
19. Weigl, B.H. and Yager, P., *Microfluidics - Microfluidic diffusion-based separation and detection*. *Science*, 1999. 283(5400): 346-347.

20. Kambolz, A.E., Weigl, B.H., Finlayson, B.A., and Yager, P., *Quantitative Analysis of Molecular Interaction in a Microfluidic Channel: the T-Sensor*. Analytical Chemistry, 1999. 71(23): 5340-5347.
21. Hatch, A., Kamholz, A.E., Hawkins, K.R., Munson, M.S., Schilling, E.A., Weigl, B.H., and Yager, P., *A rapid diffusion immunoassay in a T-sensor*. Nature Biotechnology, 2001. 19(5): 461-465.
22. Liu, R.H., Yu, Q., and Beebe, D.J., *Fabrication and characterization of hydrogel-based microvalves*. Journal of Microelectromechanical Systems, 2002. 11(1): 45-53.
23. Beebe, D.J., Moore, J.S., Yu, Q., Liu, R.H., Kraft, M.L., Jo, B.H., and Devadoss, C., *Microfluidic tectonics: A comprehensive construction platform for microfluidic systems*. Proceedings of the National Academy of Sciences of the United States of America, 2000. 97(25): 13488-13493.
24. Beebe, D.J., Moore, J.S., Bauer, J.M., Yu, Q., Liu, R.H., Devadoss, C., and Jo, B.H., *Functional hydrogel structures for autonomous flow control inside microfluidic channels*. Nature, 2000. 404(6778): 588-590.
25. Righetti, P.G., *Isoelectric Focusing: Theory, Methodology and Applications*. Laboratory Techniques in Biochemistry and Molecular Biology, ed. Work, T.S. and Work, E. Vol. 11. 1983, Amsterdam: Elsevier Biomedical Press.
26. Howard, G.C. and Brown, W.E., *Modern Protein Chemistry: Practical Aspects*. 2002: Boca Raton.
27. Creighton, T.E., *Protein Function: a Practical Approach*. Practical approach series. Vol. 175. 1997, New York: Oxford University Press Inc.
28. Ernster, L. and Kuylentierna, B., *Outer Membrane of Mitochondria*, in *Membranes of Mitochondria and Chloroplasts*, Racker, E., Editor. 1970, Van Nostrand Reinhold Company: New York.
29. Plummer, D.T., *The Electrophoretic Behaviour of Mitochondria from Kidney and Liver of Rats*. Biochem J., 1965. 96: 729.
30. Andersson, H., van der Wijngaart, W., Enoksson, P., and Stemme, G., *Micromachined flow-through filter-chamber for chemical reactions on beads*. 2000. 67(1-2): 203-208.
31. Sato, K., Tokeshi, M., Odake, T., Kimura, H., Ooi, T., Nakao, M., and Kitamori, T., *Integration of an immunosorbent assay system: Analysis of secretory human immunoglobulin A on polystyrene beads in a microchip*. 2000. 72(6): 1144-1147.